JOM
https://doi.org/10.1007/s11837-023-06123-8

NANOSTRUCTURED BIOMATERIALS

Curcumin-Laden Crosslinked Chitosan–PVA Films: The Synergistic Impact of Genipin and Curcumin on Accelerating Wound Closure

RETEESHA RAMDANI,[1] ANUSHA M. RAO,[1] MISHAL POKHAREL,[1] TARUN MATETI,[2,3] K. LIKHITH,[1] MALTI KUMARI,[2] S. SUPRIYA BHATT,[4] MANASA NUNE,[4] and GOUTAM THAKUR [1,5]

1.—Department of Biomedical Engineering, Manipal Institute of Technology, Manipal Academy of Higher Education, Manipal, Udupi, Karnataka 576104, India. 2.—Materials Research Centre, Indian Institute of Science, C. V. Raman Road, Bangalore, Karnataka 560012, India. 3.—Department of Chemical Engineering, Manipal Institute of Technology, Manipal Academy of Higher Education, Manipal, Udupi, Karnataka 576104, India. 4.—Manipal Institute of Regenerative Medicine, Manipal Academy of Higher Education, Yelahanka, Bangalore, Karnataka 560065, India. 5.—e-mail: goutam.thakur@manipal.edu

Wound dressings play a critical role in healing by maintaining a moist environment and protecting against infection. Here, we fabricate crosslinked films of chitosan–polyvinyl alcohol–genipin–curcumin to investigate the synergistic wound-healing effect of genipin and curcumin. The chemical bonding, morphology, strength, water retention capacity, curcumin release characteristics, and cytotoxicity of the films were investigated. The results showed a 192% increase in tensile strength and good water retention, and the infrared analysis and scanning electron microscopy micrographs confirmed genipin crosslinking and the presence of curcumin in the films, whose morphology was uniform and continuous. The curcumin-loaded films were found to have insignificant cytotoxicity against 3T3 fibroblast cells, proving their biocompatibility. The curcumin dissolution tests determined the amount of curcumin released from the films with time, and assessed the release characteristics to be sustained at all pH levels. In vivo trials were carried out on rodents to evaluate the wound-healing effects of the films, and the results showed that the curcumin-incorporated crosslinked films accelerated wound healing compared to the uncrosslinked and curcumin-absent films, confirming their effectiveness for wound healing.

INTRODUCTION

Injuries that break the skin or other tissues are called wounds, which may be internal or external (based on their origin); open or closed wounds (based on the cause of the wound); acute: wounds that heal in the predicted time duration[1] or chronic: or wounds that fail to heal properly and promptly with conventional time (based on the wound-healing physiology).[2]

Many factors, such as oxygen, temperature, and pH, can interfere with the healing process, leading to improper or impaired wound healing.[3] A dressing can help protect the wound from microbes and maintain a warm and moist environment to accelerate healing, absorb the exudates, and be permeable to gases and water vapor. Other dressing essentials include biocompatibility, reproducibility, flexibility, and non-toxicity. A dressing material incorporating drugs further accelerates healing.[4]

Reteesha Ramdani, Anusha M. Rao, Mishal Pokharel and Tarun Mateti contributed equally.

(Received February 13, 2023; accepted August 25, 2023)

Published online: 18 September 2023

Using degradable polymers promotes cell proliferation and integration, and is chosen for dressings because their replacement is inessential.[5] Such polymers can make hydrogels with high water retention capabilities, high flexibility, porous structures,[6] and sponges, which are often reusable and can be used for applications requiring support or cushioning.[7,8] They can also make thin polymer films, which aid in excellent skin healing,[9] as they are extremely thin and can be deposited as coatings on various surfaces and easily modified to introduce specific functionalities. Moreover, thin films easily adhere and loosen from the wound bed, conform to its contours, and can be used with secondary dressings. However, their strength is weak without crosslinkers improving their mechanical properties.[10,11]

Polyvinyl alcohol (PVA) is a biocompatible film-forming polymer with suitable physicochemical properties. As PVA is also water-soluble and non-toxic,[12] it is used in applications such as hemodialysis, artificial pancreas design, and medical implants.[13] Chitosan is a natural polysaccharide that resembles those of the extracellular matrix.[14] Chitosan applications in the commercial and biomedical fields have increased due to its low toxicity, biocompatibility with blood and tissues, and biodegradability.[15] Chitosan is used in wound and burn treatments because it accelerates the formation of fibroblasts and increases early-phase healing reactions.[16] Also, it is used to develop wound dressings such as hydrogels,[17] sponges,[18] and thin films.[19]

Chitosan can be crosslinked using various crosslinkers to enhance its stability. For example, polyethylene glycol[20] and ethylene glycol diglycidyl ether[21] form covalent bonds when introduced with functional groups, such as methacrylate or diacrylate, resulting in a crosslinked hydrogel structure. Another such compound is sodium tripolyphosphate, which forms polyelectrolyte complexes with chitosan through ionic interactions.[22] Although glutaraldehyde is commonly used to crosslink chitosan and PVA blends, it causes significant cytotoxicity. Therefore, a more biocompatible crosslinker is genipin (GP), which is much less cytotoxic than glutaraldehyde.[23] Another compound that can be used to treat wounds is curcumin (CUR), which can promote wound healing by modulating several physiological and cellular processes.[24]

Although genipin and curcumin have previously been investigated for their wound healing properties, their powerful combination remains unexplored. Herein, we prepared CS–PVA–GP films loaded with curcumin to inspect wound healing in-vivo through the synergistic effect of genipin and curcumin. The blend CS–PVA was chosen as the base because these scaffolds are porous and promote aeration of the wound site. Their amino and hydroxyl groups promote cell attachment and proliferation, retain moisture due to their hydrophilic nature, and stimulate macrophages and fibroblasts, which promote the inflammatory stage of wound healing.[25,26] We also evaluated the films' thickness, chemical bonding, morphology, strength, water retention capability, and in vitro pharmacokinetics of curcumin.

MATERIALS AND METHODS

Materials

We purchased polyvinyl alcohol, chitosan, lactic acid, and genipin from Himedia, Mumbai, India, Marine Chemicals, Kerala, India, SD Fine Chemicals, Mumbai, India, and Challenge Bioproducts, Taipei, Taiwan, respectively.[9] Curcumin was purchased from Merck, Mumbai, India. No further purification of the chemicals was required, and distilled water was used throughout this study.

Preparation of Polymer Films

The solvent-casting method[27] was adopted to fabricate thin polymer films. A 2% (w/v) chitosan solution was prepared by dissolving 2 g of chitosan in 100 ml of lactic acid, followed by slight stirring and heating to approximately 70°C. A 10% (w/v) PVA solution was prepared by dissolving 5 g of PVA in 50 ml of preheated distilled water, and was stirred for 2 h at around 80°C. The thin film preparations were carried out using different polymer ratios, as shown in Table I. The PVA solution was added to the chitosan solution dropwise, and the mixtures were stirred moderately for 30 min. The homogenous solutions were then cast onto glass plates, dried for 24–48 h at room temperature, and peeled. Figure 1 shows a CS–PVA thin film.

Film Thickness

The film thickness was recorded using a digital micrometer (Mitutoyo, Japan) with a resolution of 0.001 mm. The thickness was randomly measured on each film, and the averages and mean were calculated. Subsequently, the suitable polymer concentration ratio for crosslinking was experimentally determined based on the solubility of the polymer in their respective solvents. Chitosan at higher concentrations thickens faster than PVA, which results in poor polymer blending. In such a case, the chitosan concentration will be reduced and the PVA concentration will be increased to obtain the desired polymer matrix.[9]

Crosslinking with Genipin

The CS–PVA films were crosslinked with genipin by adding 0.5% (v/v) genipin to the CS–PVA solution and thoroughly mixed to obtain a homogenous solution. The solution was poured onto glass plates and dried at room temperature for 1–2 days. The films were peeled off upon drying and were dark blue, resulting from the spontaneous reaction of

Table I. Various polymer concentrations used in preparing CS–PVA thin films

CS–PVA ratio	Chitosan (g)	PVA (g)
1:5	17	83
2:5	28	72
3:5	38	62
4:5	44	56
5:5	50	50

CS chitosan, *PVA* polyvinyl alcohol.

Fig. 1. A CS–PVA thin film.

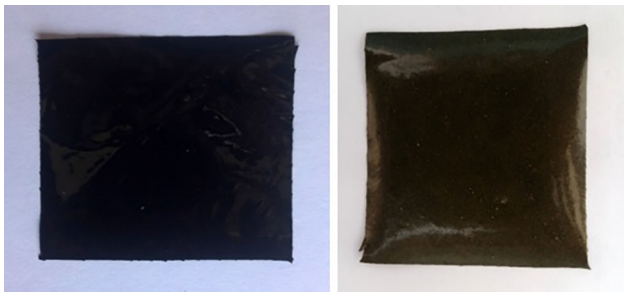

Fig. 2. Left a CS–PVA film crosslinked with genipin, right a CS–PVA–GP film integrated with curcumin.

genipin with the amino group in chitosan. Figure 2 shows a genipin crosslinked CS–PVA film.

In the other crosslinking method, CS–PVA films were prepared and allowed to dry for 1–2 days. Subsequently, they were immersed in a 0.5% (v/v) genipin solution and left to dry. After 2 days, the solution completely evaporated, and the films became bluish. However, the films had shrunk and become brittle, and were hus subsequently discarded.

Curcumin-Loading in Films

Due to the hydrophobic nature of curcumin, a suspension of PVA and curcumin was prepared. This approach ensured that the maximum curcumin was uniformly distributed within the films. An amount of 50 mg of curcumin was added to a beaker containing 10% (v/w) PVA, and the suspension was kept in a sonication bath and stirred for 20 min. The mixture of curcumin and PVA was added to the chitosan solution drop-by-drop, kept on a magnetic stirrer, and stirred moderately for 30 min. Subsequently, sonication was used to remove the trapped bubbles, and genipin was added to the mixture. The mixture was then poured onto glass plates, dried for 24–48 h at room temperature, and peeled. Figure 2 shows a CS–PVA–GP film integrated with curcumin.

Strength Analysis

The tensile strength and elongation of the films were recorded using a universal testing machine (Instron 3366). Film strips of dimensions 3 cm × 1 cm held 30 mm apart by clamps were pulled with a top clamp at 5 mm/min, and the percentage of elongation and tensile strength were calculated using Eqs. 1 and 2, respectively:[9]

$$\%\ \text{Elongation} = \frac{E_f - E_i}{E_i} \times 100 \qquad (1)$$

where E_f is the final length of the sample (at rupture), and E_i is the initial length of the sample.

$$\text{Tensile Strength(MPa)} = \frac{\text{Force at break(kg)} \times 9.8\left(\frac{m}{s^2}\right)}{\text{Thickness (mm)} \times \text{Width (mm)}} \times 100 \qquad (2)$$

Swelling Studies

The CS–PVA, CS–PVA–GP, and CS–PVA–GP–CUR films were cut into tiny pieces to determine the initial dry weight. The films were then submerged in water and weighed on an electronic balance at different intervals after removing water from their surface. This process was continued until a constant weight was obtained, and the swelling percentage was calculated using:[9]

$$\%\text{Water retention} = \frac{w_t - w_0}{w_0} \times 100 \qquad (3)$$

where w_t is the weight of the samples immersed in water at different intervals of time and w_0 is the initial weight of the samples.

Infrared Spectroscopy Analysis

An infrared (IR) spectrophotometer (Shimadzu IR-83400) was utilized to analyze the chemical bonding and film composition. IR analysis was performed for chitosan, genipin, curcumin, PVA,

uncrosslinked CS–PVA films, CS–PVA–GP films, and CS–PVA–GP–CUR films.

Morphology Analysis

The morphology of the CS–PVA–GP and CS–PVA–GP–CUR films was analyzed using a field-emission scanning electron microscope (FE-SEM; Ultra55; Zeiss, Germany). The films were placed on aluminum specimen mounts with double-sided adhesive tape. The specimen mounts were then coated with silver using a sputter coater. The films were then examined under FE-SEM using a × 500 magnification and a 20-kV accelerating voltage to perceive their microstructure. The average particle size was calculated using ImageJ, and the elemental analysis of the CS–PVA–GP–CUR films was performed using energy-dispersive X-ray spectroscopy (EDS).

In Vitro Curcumin Release Studies

Standard solutions of different concentrations of curcumin (2–10 μg/ml) were prepared. The absorbance of each of these solutions was measured using a UV–Vis spectrophotometer (Labline Instruments, India). A graph between concentration and absorbance was plotted to generate the calibration curve. Then, the curcumin dissolution tests were performed to understand the curcumin release pattern.

For the curcumin release studies, the CS–PVA–GP–CUR films were cut into small pieces of 5 cm × 5 cm and placed in beakers containing phosphate buffer solution of pH 6.5, 7.4, and 8.5, respectively, which acted as the release medium. A magnetic stirrer was used to constantly mix the solution at a low rpm. Then 4 ml was withdrawn from the beakers at different intervals. To maintain the sink conditions, 4 ml of fresh phosphate buffer was added to the dissolution medium each time. The absorbance of the withdrawn sample was analyzed using the UV–Vis spectrophotometer and the concentration of each sample was determined by relating its absorbance to the calibration curve. The cumulative percentage release of curcumin was calculated using:[28]

$$\%\text{Cumulative release} = \frac{\text{Cumulative amount of curcumin released}}{\text{Total curcumin loaded into the film}} \times 100 \quad (4)$$

Cytotoxicity Assessment

An MTT assay was used to determine the cell viability. The 3T3 cells were grown in the CS–PVA, CS–PVA–GP, and CS–PVA–GP–CUR films for 1 days, 3 days, and 5 days. Then, 0.5 mg/ml of MTT was added to the films and incubated for 4 h at 37°C and 5% CO_2. The formazan precipitates in the films were dissolved in DMSO, and the absorbance was measured using a multimode microplate reader (Ensight HH34000000; Perkin Elmer).

A live/dead viability kit (Thermo Fisher, USA) was used to visualize the 3T3 cell viability when exposed to the CS–PVA, CS–PVA–GP, and CS–PVA–GP–CUR film environments. The materials used were disinfected using ultraviolet irradiation before cell seeding. The wells were incubated for 1 h at 37°C with a stock solution of calcein-AM and ethidium homodimer-1. Calcein-AM, a cell-permeable dye, is transformed into a green fluorescent calcein by live cells, while ethidium homodimer-1 attaches to the nucleic acids of cells with compromised membranes to create red fluorescence. A fluorescent microscope (Eclipse-TE2000-U; Nikon) was used to capture the images.

In Vivo Studies

The aim of the in vivo studies is to evaluate the wound-healing properties of the different types of chitosan–PVA films on rodent models. In this study lasted for 21 days, and adult female albino Wistar rats weighing 150–210 g were selected because they are convenient to handle, readily available, and resistant to infection. The rats were placed in separate cages without husks, and food and water were provided ad libitum. The experiment was approved and carried out at Manipal Academy of Higher Education, Manipal, similar to our previous study.[9]

The excision wound model evaluated the wound-healing activity. A total of 18 rats were divided into three groups: 6 for the control group, 6 for the crosslinked film without curcumin (Group I), and 6 for the crosslinked film with the curcumin (Group II). The animals were named as follows: control group (A1, A2, A3, A4, A5, A6), Group I (G1, G2, G3, G4, G5, G6), and Group II (C1, C2, C3, C4, C5, C6).

The rats were anesthetized with 0.25 mg of ketamine and placed on the operating table. Their fur was shaved in the dorsal position, and the wound area was marked on their back. A circular wound of area 4.90 cm^2 was excised, and, after the bleeding stopped, the wound was blotted with sterile gauze. No films were applied to the control group, while the respective films were placed on the wound in the treatment groups (Group I and Group II). The films were prepared and stored per our previous study.[9]

The changes in the wound size were measured regularly. For visual comparison, photographs were taken at specific intervals. The wound area and the wound contraction were calculated to find the degree of reduction in the wound area at different periods.[9]

Statistical Analysis

All the experiments were carried out in triplicate, and the results were recorded as the arithmetic mean ± standard deviation. One-way analysis of variance (GraphPad Prism 7 Software, La Jolla, USA) was used to perform the statistical analysis, and a p value < 0.05 was considered statistically significant.

RESULTS AND DISCUSSION

Physio-Morphological Properties

Film Thickness

The average thickness of the prepared films ranged from 30 μm to 85 μm. Among the films, CS–PVA (4:5) was considered the best for crosslinking (which is supported by our previous work[9]), and genipin crosslinking produced uniform films. The average thicknesses of the CS–PVA, CS–PVA–GP, CS–PVA–GP–CUR films were 73.8 ± 10 μm, 45.7 ± 20 μm, and 70 ± 20 μm, respectively. The decrease in thickness of the CS–PVA–GP films can be attributed to the effect of genipin crosslinking, making the films shrink and compact by bonding with the amino groups of chitosan to form short-chain polymer networks,[29] and the increase in the thickness of the CS–PVA–GP–CUR films compared to the CS–PVA–GP films can be attributed to the additional curcumin component in the films.

Infrared Spectroscopy Analysis

IR spectroscopy was used to investigate the polymer bonding, genipin crosslinking, and curcumin incorporation, as shown in Fig. 3.

The spectrum of chitosan powder (refer to online supplementary material Figure S1) was obtained in 400–4000 cm^{-1}. The peaks at 1392.13 cm^{-1}, 1539.15 cm^{-1}, and 1691.67 cm^{-1} indicate C=O bonding, which shifts to 1432–1643 cm^{-1} in the CS–PVA films. The peak at 3578.75 cm^{-1} corresponds to O-H bonding, and at 3195.06 cm^{-1} corresponds to N-H bonding.[30] These results are consistent with our earlier research, which found that the distinctive chitosan membrane peaks were located at 1586 cm^{-1}, 1657 cm^{-1}, and 1321 cm^{-1}.[9]

The peak at 3917 cm^{-1} in the PVA spectrum (Figure S1) indicates O-H bonding due to inter- and intramolecular hydrogen interactions between chitosan and PVA,[31] which shifts to 3560 cm^{-1} in the CS–PVA films. The peak at 1713 cm^{-1} indicates C=O bonding and the band observed at 2909 cm^{-1} indicates C-H bonding from the alkyl groups.[31]

In the genipin spectrum (Figure S1), the peak at 1641.74 cm^{-1} indicates C=O bonding.[31] Genipin displays an N-H bond at 3176.81 cm^{-1} and an amine bond at 1547.6 cm^{-1}. The peaks differ from those of curcumin due to the formation of covalent bonds that consume the amine groups in pure chitosan.[31]

The curcumin spectrum (Figure S1) peaks around 3000 cm^{-1}, indicating phenolic O-H bonding. The peak at 1627 cm^{-1} indicates C=C aromatic bonding; 1507 cm^{-1} for C=O and C=C bonding; 1423 cm^{-1} for olefinic O-H bonding; 1275 cm^{-1} for C-O aromatic bonding; and 1028 cm^{-1} for C-O-C bonding.[32–34]

A rearrangement of molecular chains for covalent bonding occurs when chitosan is crosslinked with genipin. The peak heights at 846 cm^{-1} and 1058 cm^{-1} changed, indicating inter- and intramolecular bonding of the crosslinkers. The new peaks indicate that crosslinking has occurred in the films.

The IR spectrum of the CS–PVA–GP–CUR films is similar to that of the CS–PVA–GP films, where additional peaks or characteristic peaks of curcumin are absent upon adding it to the CS–PVA–GP films. Thus, no chemical bonding has occurred between curcumin and the crosslinked films, and it is a suspension.

Morphology Analysis

The surface morphology of the films was studied using SEM. Figure 4 shows the SEM micrographs of the CS–PVA, CS–PVA–GP, and CS–PVA–GP–CUR films. The surface of the CS–PVA films was smooth, continuous, and uniform, while the CS–PVA–GP films had an irregular surface, indicating genipin crosslinking. The SEM micrograph of the CS–PVA–GP–CUR films shows curcumin particles that have an average size of 3.128 μm dispersed within the film matrix, supported by the EDS elemental analysis. Although curcumin agglomeration causes the formation of larger particles and is evidenced in the literature on other subjects to adversely affect properties,[35–37] the curcumin particles in our films are randomly dispersed, due to which the films can be considered quasi-homogenous, with an excess of

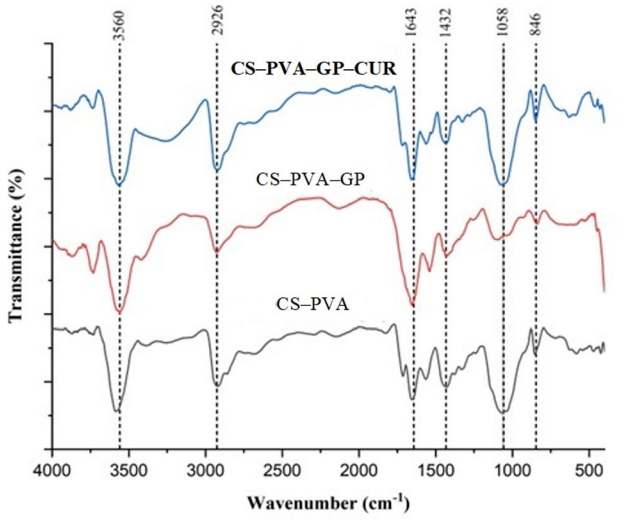

Fig. 3. The IR spectra of CS–PVA–GP–CUR, CS–PVA–GP, and CS–PVA films, depicting various functional groups.

recrystallized curcumin visible on the film surface. None of the films had cracks, tears, or folds.

Mechanical Properties

Strength Analysis

The mechanical strength of the CS–PVA and CS–PVA–GP films was measured in terms of the maximum tensile strength (MPa) and extension (mm). The mechanical strength shows the ability of the films to resist breaking under tensile stress, while the extension shows the ductility of the films. These characteristics reveal the strength and elasticity of the films. The tensile strength and extension of the CS–PVA films were 18.53 MPa and 24.82 mm; the CS–PVA–GP films were 27.99 MPa and 11.77 mm; and the CS–PVA–GP–CUR films were 54.11 MPa and 9.14 mm. Figure S2 shows the stress–strain curves of the CS–PVA, CS–PVA–GP, and CS–PVA–GP–CUR films.

The CS–PVA–GP films had better mechanical properties than the uncrosslinked films. The CS–PVA–GP–CUR films possessed the greatest tensile strength, with an increase of 192% compared to the uncrosslinked films, which showed 171% more extension, indicating flexibility. The improvement in tensile strength of the CS–PVA–GP–CUR films can be attributed to the high tensile properties and crystallinity of curcumin[38] and the film compactness after crosslinking.

Swelling Studies

The uncrosslinked and crosslinked films showed significant differences in their swelling capabilities. The CS–PVA films were more porous than the CS–PVA–GP and CS–PVA–GP–CUR films and thus their water uptake capability was superior to the crosslinked films. Figure 5 shows the percentage degree of swelling of the CS–PVA, CS–PVA–GP, and CS–PVA–GP–CUR films.

The water content of the CS–PVA–GP and CS–PVA–GP–CUR films increased for 15 min, remaining almost constant and reaching saturation afterward. These results prove that genipin crosslinks with chitosan/PVA at a high degree and forms a more compact structure, thus possessing inferior water-holding capabilities. Moreover, such films can retain water for longer without destroying their structure. Therefore, genipin crosslinked films are better suited for wound-healing applications, as they can absorb the excessive exudates from wounds and help maintain good moisture levels.

Cytotoxicity Assessment

The cytotoxicity of the films was evaluated using an MTT assay using 3T3 fibroblast cells. Figure 6 shows the % cell viability of the CS–PVA, CS–PVA–GP, and CS–PVA–GP–CUR films after 24 h, 72 h, and 120 h, respectively. The CS–PVA–GP and CS–PVA–GP–CUR films had insignificant cytotoxicity against 3T3 fibroblast cells, maintaining nearly 100% cell viability on all test days. This shows that the CS–PVA–GP and CS–PVA–GP–CUR films are biocompatible and is further substantiated by the live/dead cell imaging taken after 1 days, 3 days, and 5 days of culture (Fig. 7). and these results are within the acceptable limits according to ISO 10993-5-2009.[39]

Wound-Healing Properties

Cumulative Curcumin Release

The maximum absorbance wavelength (λ_{max}) of curcumin was found to be 430 nm. The absorbance of different concentrations of the curcumin solution was measured in triplicate, and the average and standard deviation were calculated (Table S1). The calibration curve (Figure S3) was plotted using these values to show the change in absorbance with different concentrations of the curcumin solution and to calculate the unknown concentration of the withdrawn sample in the curcumin release studies at varying pH levels.

The absorbance of the withdrawn samples was related to their respective curcumin concentration using the calibration curve (Table S2). Figure 8 shows the graph of the cumulative curcumin release plotted over time at varying pH levels. The curcumin release pattern at a neutral pH shows an initial burst release, and, with an increase in time, the release from the CS–PVA–GP–CUR films gradually decreases and adopts a sustained release behavior after approximately 10 h. Interestingly, such behavior was maintained even at acidic and basic pH levels, indicating that the pH changes did not affect the films' curcumin release characteristics! Thus, the films maintained a constant level of curcumin (zero order dissolution) for an extended period, ensuring curcumin bioavailability throughout any wound-healing process.

In Vivo Study

Figure 9 shows the % wound contraction in the rats, and Fig. 10 shows the gradual wound healing in the rats of different groups on days 1, 5, 10, 14, and 21. Rapid epithelialization was found in the photographs of wounds treated with the films, indicating better wound healing than for the untreated wounds. This indicates that genipin accelerated wound healing. Scabs were absent in Group I and Group II, showing that the films provided a moist environment for the healing process. Moreover, it can be seen that, in Group II, the wound-healing rate was faster than in Group I due to the release of curcumin from the films. Although Group II had the highest inflammation on day 3, it reduced faster than in Group I and Group II due to the anti-inflammatory properties of curcumin. The synergistic wound-healing effect of genipin and curcumin can be observed since the

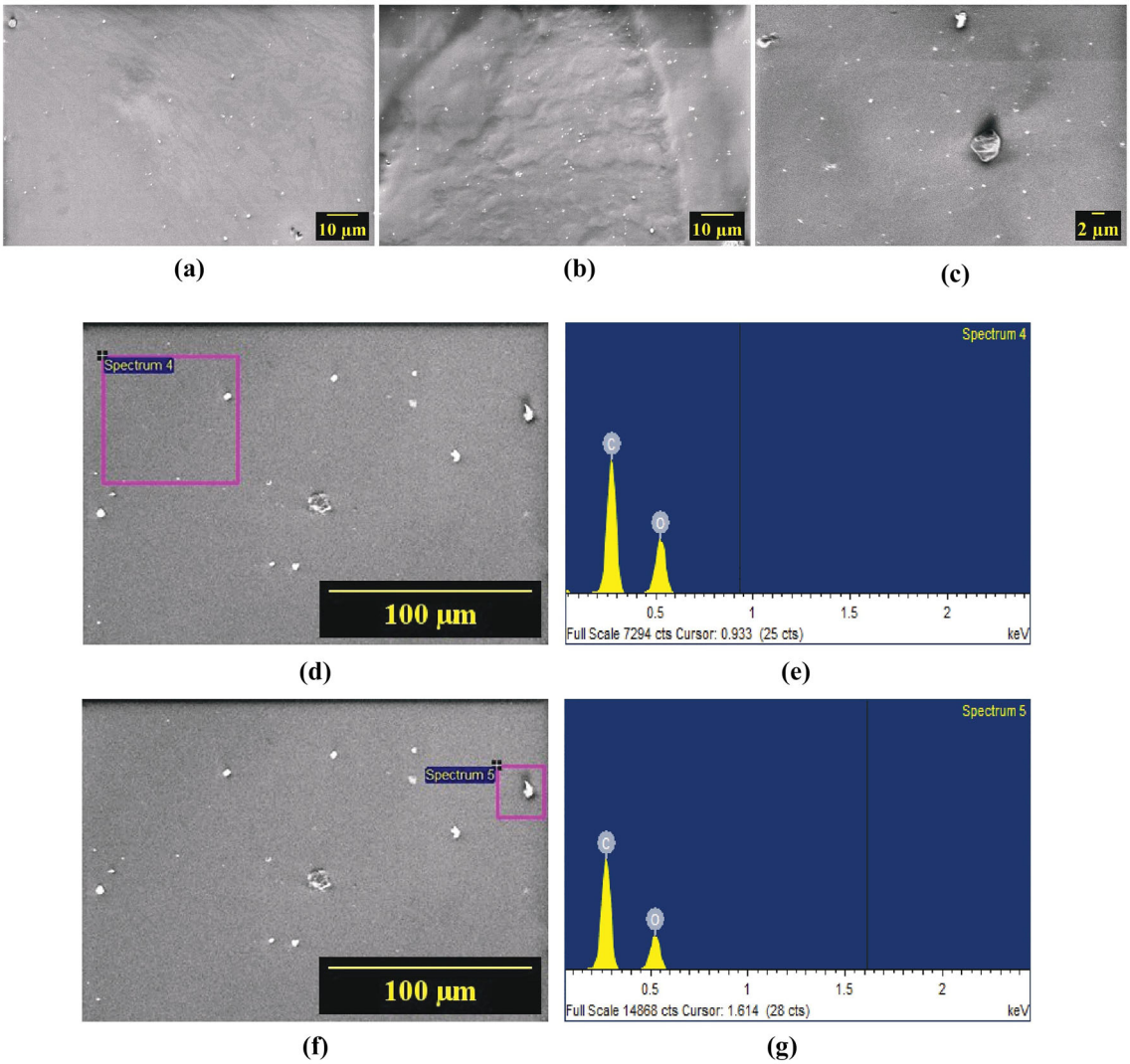

Fig. 4. SEM micrographs of (a) CS–PVA film, (b) CS–PVA–GP film, and (c) CS–PVA–GP–CUR films, depicting the films' morphology and curcumin particles. (d, e) and (f, g) is the elemental analysis of the particles on the CS–PVA–GP–CUR films' surface performed using EDS.

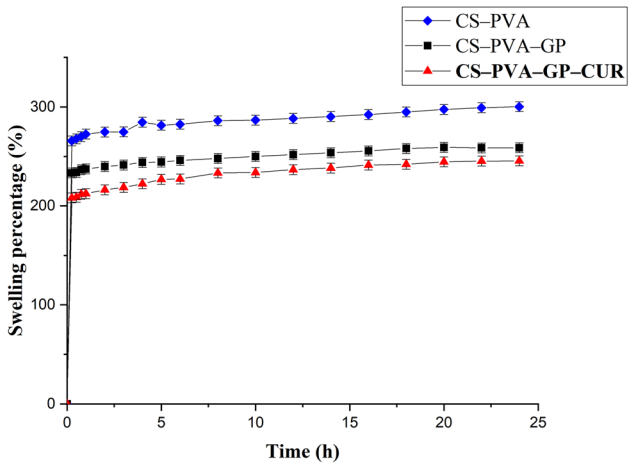

Fig. 5. Swelling index profiles of the CS–PVA, CS–PVA–GP, and CS–PVA–GP–CUR films, respectively.

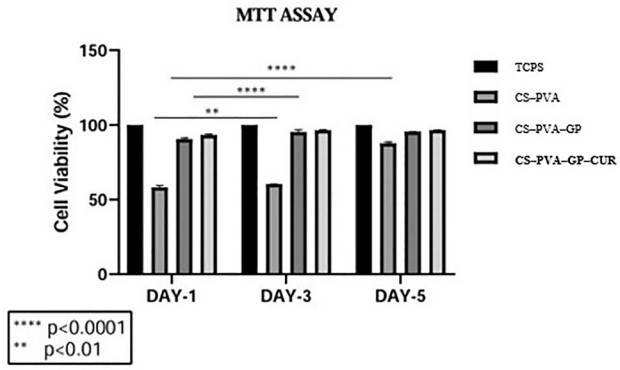

Fig. 6. 3T3 % cell viability of CS–PVA, CS–PVA–GP, and CS–PVA–GP–CUR films; each value is expressed as mean ± SD, $n = 3$ independent experiments.

wound area was dramatically reduced and always smaller than in Group I and Group II. Although the precise tracking of the wound area from day 14

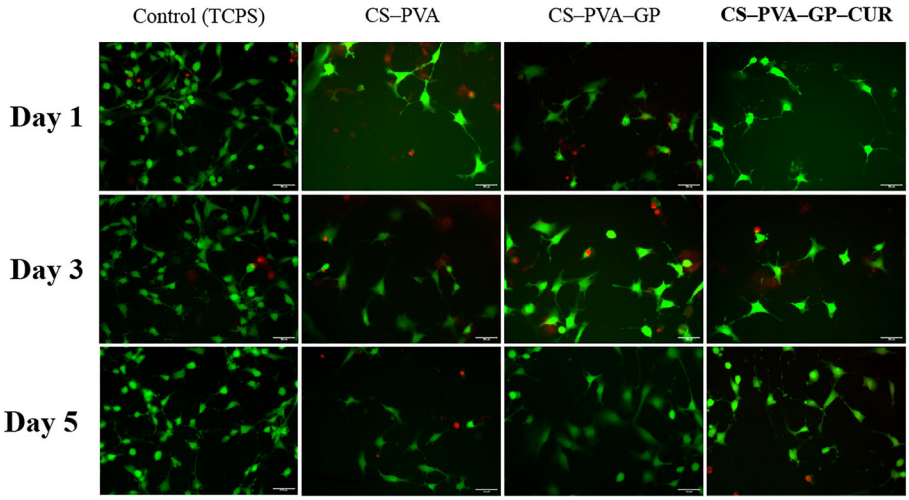

Fig. 7. Live/dead assay of 3T3 fibroblast cells cultured on CS–PVA, CS–PVA–GP, and CS–PVA–GP–CUR films after 1 days, 3 days, and 5 days.

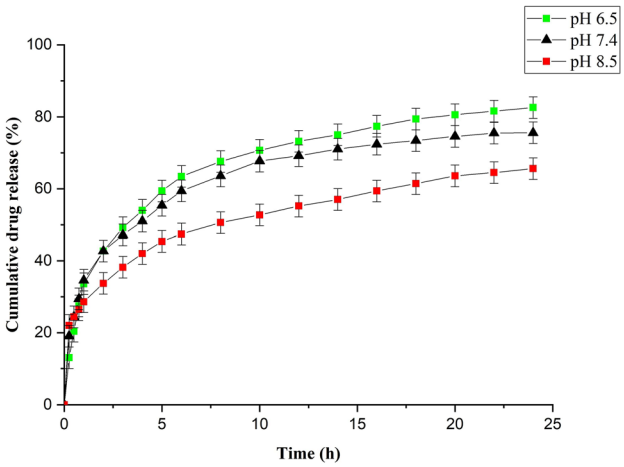

Fig. 8. In vitro curcumin release profile of the CS–PVA–GP–CUR films at varying pH levels.

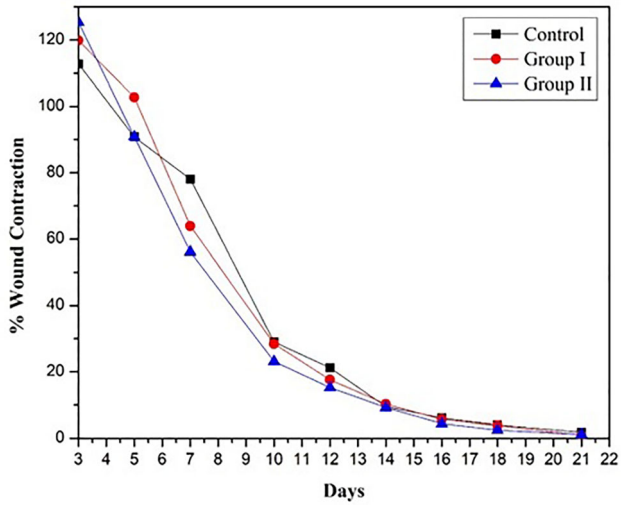

Fig. 9. % Wound contraction in the rats of different groups across 21 days.

onwards became a challenge, a separation can be observed between the wound-healing curves of Group I and Group II, and the synergistic wound-healing effect of genipin and curcumin would be more pronounced if the wound area of all the groups were larger than in this study. Interestingly, this wound closure rate was much faster than in our previous study,[9] indicating the role of curcumin in enhancing wound healing. The % wound contraction values corresponding to Fig. 9 are provided in Table S3.

Curcumin influences cutaneous wound healing by contributing to tissue remodeling, blood cell formation, and collagen synthesis.[15] Concerning the inflammatory phase, curcumin reduces inflammation by inhibiting the expression of pro-inflammatory proteins and promoting the production of anti-inflammatory proteins.[40] Curcumin also ameliorates the proliferative phase by decreasing the number of collagen-breaking enzymes, promoting the maturity of collagen fibers, and mediating fibroblasts into wound sites in vivo, leading to their subsequent differentiation into myofibroblasts,[41–43] marking the start of wound contraction. Furthermore, curcumin reduces the epithelialization period, induces apoptosis during the early phase of wound healing, and accelerates the healing process by shortening the inflammatory phase.[43] Thus, when wounds are treated with curcumin and genipin (an anti-inflammatory agent that initiates early wound contraction[9]), a synergistic healing effect is produced, resulting in rapid wound closure, as seen in this study.

CONCLUSION

This study aimed to develop curcumin-based CS–PVA films crosslinked with genipin for wound-healing applications. As polymer films usually have

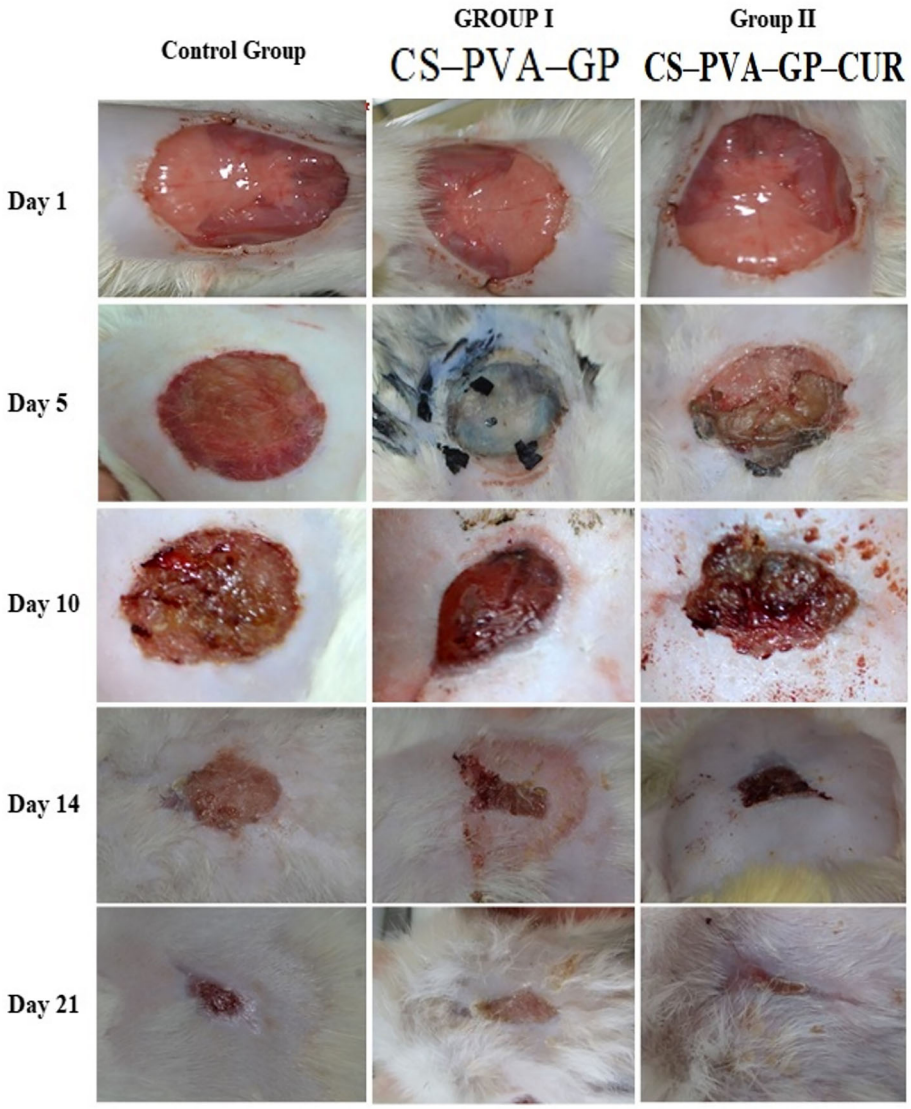

Fig. 10. Wound-healing progression images of albino Wistar rats of different groups on different days.

poor mechanical strength, genipin was used as a crosslinker. The films developed were characterized for their mechanical strength, water retention, curcumin release characteristics, and cytotoxicity. Infrared spectroscopy analysis confirmed crosslinking due to inter- and intramolecular bonding, and the SEM micrographs confirmed the presence of curcumin and uniformity of the films with a continuous morphology. The strength analysis showed that the genipin crosslinked films had high tensile strength. The curcumin release studies showed a sustained release profile at all pH levels after an initial burst release from the film. The films were noncytotoxic against 3T3 fibroblast cells, proving their biocompatibility. In vivo studies were performed on albino Wistar rats to assess the healing effects of the films on a wound. The application of curcumin-based films showed promising results, with the rats in Group II showed faster healing than those in the other groups. In conclusion, genipin crosslinked curcumin films accelerated wound healing, leading to faster wound closure.

SUPPLEMENTARY INFORMATION

The online version contains supplementary material available at https://doi.org/10.1007/s11837-023-06123-8.

FUNDING

Open access funding provided by Manipal Academy of Higher Education, Manipal.

CONFLICT OF INTEREST

The authors have no conflicts of interest to declare.

OPEN ACCESS

REFERENCES

1. N.J. Percival, *Surg. Infect. (Larchmt.)* 20, 114 (2002).
2. K. Moore, R. McCallion, R.J. Searle, M.C. Stacey, and K.G. Harding, *Int Wound J* 3, 89 (2006).
3. S. Guo and L.A. DiPietro, *J. Dent. Res.* 89, 219 (2010).
4. S. Dhivya, V.V. Padma, and E. Santhini, *Biomedicine (Taipei)* 5, 24 (2015).
5. M.S. Shoichet, *Macromolecules* 43, 581 (2010).
6. Y. Liang, J. He, and B. Guo, *ACS Nano* 15, 12687 (2021).
7. K. Zhang, X. Bai, Z. Yuan, X. Cao, X. Jiao, Y. Li, Y. Qin, Y. Wen, and X. Zhang, *Biomaterials* 204, 70 (2019).
8. A. Sathiyaseelan, K. Saravanakumar, A.V.A. Mariadoss, and M.H. Wang, *Antibiotics* 10, 524 (2021).
9. R. Panchal, T. Mateti, K. Likhith, F.C. Rodrigues, and G. Thakur, *React. Funct. Polym.* 178, 105339 (2022).
10. H. Chopra, S. Bibi, S. Kumar, M.S. Khan, P. Kumar, and I. Singh, *Gels* 8, 111 (2022).
11. N.O. Dogan, U. Bozuyuk, P. Erkoc, A.C. Karacakol, A. Cingoz, F. Seker-Polat, M.A. Nazeer, M. Sitti, T. Bagci-Onder, and S. Kizilel, *Adv. Nanobiomed. Res.* 2, 2100033 (2022).
12. K.S. Pavithra, S.C. Gurumurthy, M.P. Yashoda, T. Mateti, K. Ramam, R. Nayak, and M.S. Murari, *J. Therm. Anal. Calorim.* 146, 601 (2021).
13. A. Kumar and S.S. Han, *Int. J. Polym. Mater. Polym. Biomater.* 66, 159 (2017).
14. K. Balagangadharan, S. Dhivya, and N. Selvamurugan, *Int. J. Biol. Macromol.* 104, 1372 (2017).
15. B. Joe, M. Vijaykumar, and B.R. Lokesh, *Crit. Rev. Food Sci. Nutr.* 44, 97 (2010).
16. W. Paul and C.P. Sharma, *Trends Biomater. Artif. Organs* 18, 18 (2004).
17. T. Mateti, L. K, A. Laha, and G. Thakur, *Curr. Opin. Biomed. Eng.* **25**, (2023).
18. R. Shakiba-Marani and H. Ehtesabi, *Int. J. Biol. Macromol.* 224, 831 (2023).
19. B.P. Genesi, R. de Melo Barbosa, P. Severino, A.C.D. Rodas, C.M.P. Yoshida, M.B. Mathor, P.S. Lopes, C. Viseras, E.B. Souto, and C. Ferreira da Silva, *Int. J. Pharm.* 634, 122648 (2023).
20. A.R. Kulkarni, V.I. Hukkeri, H.W. Sung, and H.F. Liang, *Macromol. Biosci.* 5, 925 (2005).
21. S. Bratskaya, Y. Privar, D. Nesterov, E. Modin, M. Kodess, A. Slobodyuk, D. Marinin, and A. Pestov, *Biomacromol* 20, 1635 (2019).
22. F.M. Hsieh, C. Huang, T.F. Lin, Y.M. Chen, and J.C. Lin, *Process Biochem.* 43, 83 (2008).
23. A. Bigi, G. Cojazzi, S. Panzavolta, N. Roveri, and K. Rubini, *Biomaterials* 23, 4827 (2002).
24. S. Mitra, T. Mateti, S. Ramakrishna, and A. Laha, *JOM* 74, 3392 (2022).
25. S. Ahmed and S. Ikram, *Achiev. Life Sci.* 10, 27 (2016).
26. S.G. Jin, *Chem. Asian J.* 17, e202200595 (2022).
27. E.A. El-Hefian, M.M. Nasef, and A.H. Yahaya, *J. Chem.* 8, 91 (2011).
28. J. Pang, Y. Luan, F. Li, X. Cai, J. Du, and Z. Li, *Int. J. Nanomed.* 6, 659 (2011).
29. A. Ali and S. Ahmed, in *Polymers for Food Applications* (Springer, New York, 2018), pp. 551–589.
30. I. Migneault, C. Dartiguenave, M.J. Bertrand, and K.C. Waldron, *Biotechniques* 37, 790 (2004).
31. V.M. Bispo, A.A.P. Mansur, E.F. Barbosa-Stancioli, and H.S. Mansur, *J. Biomed. Nanotechnol.* 6, 166 (2010).
32. E.H. Ismail, D.Y. Sabry, H. Mahdy, and M.M.H. Khalil, *J. Sci. Res.* 6, 509 (2014).
33. X. Chen, L.Q. Zou, J. Niu, W. Liu, S.F. Peng, and C.M. Liu, *Molecules* 20, 14293 (2015).
34. M.M. Yallapu, M. Jaggi, and S.C. Chauhan, *Colloids Surf. B Biointerfaces* 79, 113 (2010).
35. S. Al Khateeb and T.D. Sparks, *J Mater Res* 34, 2456 (2019).
36. S. Al-Khateeb, D. Pavlopoulos, T.W. Button, and J.S. Abell, *J. Supercond. Nov. Magn.* 25, 1823 (2012).
37. S. Al Khateeb, T.W. Button, and J.S. Abell, *Supercond. Sci. Technol.* 23, 095001 (2010).
38. Y. Liu, Y. Cai, X. Jiang, J. Wu, and X. Le, *Food Hydrocoll.* 52, 564 (2016).
39. M.P. Balasubramaniam, P. Murugan, D. Chenthamara, S.G. Ramakrishnan, A. Salim, F.H. Lin, B. Robert, and S. Subramaniam, *Mater. Today Commun.* 25, 101510 (2020).
40. M. Barchitta, A. Maugeri, G. Favara, R.M. San Lio, G. Evola, A. Agodi, and G. Basile, *Int. J. Mol. Sci.* 20, 1119 (2019).
41. W.M. Petroll, H.D. Cavanagh, P. Barry, P. Andrews, and J.V. Jester, *J. Cell. Sci.* 104, 353 (1993).
42. Z. Qian, M. Dai, X. Zheng, X. Xu, X. Kong, X. Li, G. Guo, F. Luo, X. Zhao, and Y.Q. Wei, *J. Biomed. Biotechnol.* 2009, 56 (2009).
43. C. Mohanty, M. Das, and S.K. Sahoo, *Mol. Pharm.* 9, 2801 (2012).